Enhanced reflection from inverse tapered nanocone arrays

Kong, Xiang-tian; Butt, Haider; Yetisen, Ali K.; Kangwanwatana, Chuan; Montelongo, Yunuen; Deng, Sunan; Cruz Vasconcellos, Fernando Da; Qasim, Malik M.; Wilkinson, Timothy D.; Dai, Qing

DOI:
10.1063/1.4892580

Enhanced reflection from inverse tapered nanocone arrays

Xiang-Tian Kong[1], Haider Butt[2]*, Ali K. Yetisen[3], Chuan Kangwanwatana[4], Yunuen Montelongo[4], Sunan Deng[2], Fernando da Cruz Vasconcellos[3], Malik M. Qasim[4], Timothy D. Wilkinson[4], Qing Dai[1]*

[1] *National Center for Nanoscience and Technology, Beijing 100190, China*

[2]*School of Mechanical Engineering, University of Birmingham, Edgbaston, Birmingham B15 2TT, UK*

[3]*Department of Chemical Engineering and Biotechnology, University of Cambridge, Tennis Court Road, Cambridge CB2 1QT, UK*

[4]*Electrical Engineering Division, Department of Engineering, University of Cambridge, Cambridge CB3 0FA, UK*

We computationally and experimentally demonstrate enhanced reflection effects displayed by silicon-based inverted nanocone arrays. A 3D finite element model is used to characterize the optical properties of the nanocone arrays with respect to the change in polarization and incident angles. The nanocone arrays are fabricated by e-beam lithography in hexagonal and triangular geometries with a lattice constant of 300 nm. The fabricated devices show a two-fold increase in reflection compared with bare silicon surface, as well as a strong diffraction within the visible and near-infrared spectra. The nanocone arrays may find a variety of applications from optical devices to energy conservation technologies.

KEYWORDS: Enhanced reflection, silicon nanocones, diffraction, e-beam lithography

Silicon (Si) nanopillars (NPs) have been the focus of enormous research in past few decades and a myriad of photonics applications have been reported.[1] With the advancements in nanofabrication, the nanopillars can be produced in periodic arrays with dimensions of the order of wavelength of light. Such arrays of tapered or cone-shaped Si nanopillars have been utilized for producing antireflection coatings,[2] and enhancing the absorption capacity of silicon-based

* Email: h.butt@bham.ac.uk, Tel: +441214158623
Email: daiq@nanoctr.cn, Tel: +86 10 82545720;

surfaces and photovoltaic devices.[3] Due to the index profile variation across height of the nanocones (NCs), light propagating through their 2D lattice is refracted downward toward the cones' bases, where the effective refractive index is higher. We previously demonstrated the reverse phenomenon of enhancing the reflection of light by using Si-based nanocones.[4] The simulated and measured wave propagation across a square periodic array of inverted cones suggested that most of the impinging radiations is reflected back from the surface. This enhanced reflection effect can be utilized for producing many practical applications such as color filters, in photovoltaics and on the surfaces of windows to back reflect infrared radiations to control heating losses in buildings.

Here, we report enhanced reflection effects displayed by the hexagonal and triangular lattice periodic arrays of inverted silicon nanocones. Arrays of inverted nanocones having radii of the order 50 nm and the lattice constants of 300 nm are characterized computationally and experimentally. Computational modeling shows that these high-density arrays display enhanced reflection effects within the visible and near-infrared (Vis/NIR) spectra. Optical measurements of the fabricated device shows enhanced reflection of order two times higher than bare Si.

In order to understand the optical properties and optimize the configuration of Si NPs, computational modeling of periodic arrays of Si NPs was performed. The "RF Waves application" mode of COMSOL Multiphysics® was chosen to model the transverse electric (TE) and transverse magnetic (TM) modes of wave propagation through the triangular and hexagonal arrays of inverse tapered silicon nanopillars. Due to the tapered shape, a three dimensional (3D) model was designed. The optical properties of the tapered silicon structures on light reflectance were studied in terms of incident angle, free space wavelength, and light polarization.

Figures 1(a, b) illustrate the model geometries of the hexagonal and triangular arrays. The radius of the top surface of the silicon cone, the height and the lattice constant were set to 50, 1000, and 300 nm, respectively. The cones were extruded with the rate of 0.4, i.e., the radius of the bottom base of the inverted cone was 20 nm. The simulations were carried out in one cubic cell (shown with red edges in Fig. 1(a, b)) for each array, utilizing the symmetry of the structures. Light was obliquely illuminated on the arrays from the top boundaries. According to the definitions of the incident angle θ and azimuthal angle ϕ shown in Fig. 1(c), the Cartesian components of the wavevector are given by

$$k_x = k_0 \sin\theta\cos\phi, k_y = k_0 \sin\theta\sin\phi, k_z = k_0 \cos\theta.$$

For polarization angle of χ, the components of electric field are given by

$$E_x = E\cos\chi\cos\theta\cos\phi - E\sin\chi\sin\phi$$
$$E_y = E\cos\chi\cos\theta\sin\phi + E\sin\chi\cos\phi$$
$$E_z = -E\cos\chi\sin\theta$$

The polarization angle χ of 0° and 90° represented the TM and TE mode of light, respectively. The azimuthal ϕ angle was set to 0 throughout the simulations. Like the pillars, the substrate material was defined as silicon. The permittivity of silicon in the visible and near infrared is fitted from empirical data cited from Palik *et. al* ,[5] given by the Herzberger-type dispersion formula:

$$n = A + BL + CL^2 + D\lambda^2 + E\lambda^4$$

where $L = 1 / (\lambda^2 - 0.101)$, $A = 3.5025$, $B = 0.1235$, $C = -1.5469\times10^{-4}$, $D = -0.0779$, and $E = 0.02$.

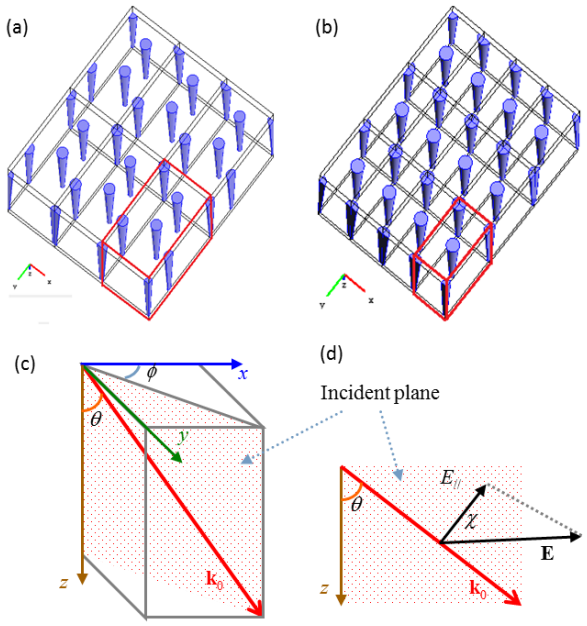

Fig. 1. Schematic of hexagonal (a) and triangular (b) arrays of inverse tapered silicon nanopillars. The cubes confined by the red edges show the simulated regions. (c) Definitions of direction angles θ(incident) and ϕ(azimuthal). (d) Definition of polarization angle χ, which is

the angle from electric field polarization with respect to the incident plane of light.

Figures 2(a, b) illustrate the simulated reflectance of hexagonal arrays of tapered silicon pillars in terms of incident angle θ and light wavelength for polarization angle χ of 0°and 90°, respectively. Figures 2(c, d) show the same for triangular arrays of tapered silicon pillars for the two polarizations. At lower incident angles ($\theta > 20°$), minimal reflection was observed from both the arrays, as the light propagation direction was almost parallel to the axis of the nanopillars, and there is not much interaction. For both the polarizations, high reflection of light (> 0.6) was observed at large incident angles ($\theta > 60°$). As the arrays are periodic, they act as diffraction grating.[6] Several diffraction orders of light were also observed which blue shift with the increase in the incidence angle. Diffraction was effected by the lattice spacing observed by the incident light. As the incident angles increased, the effective lattice spacing decreased due to which smaller wavelengths are diffracted (blue shift).

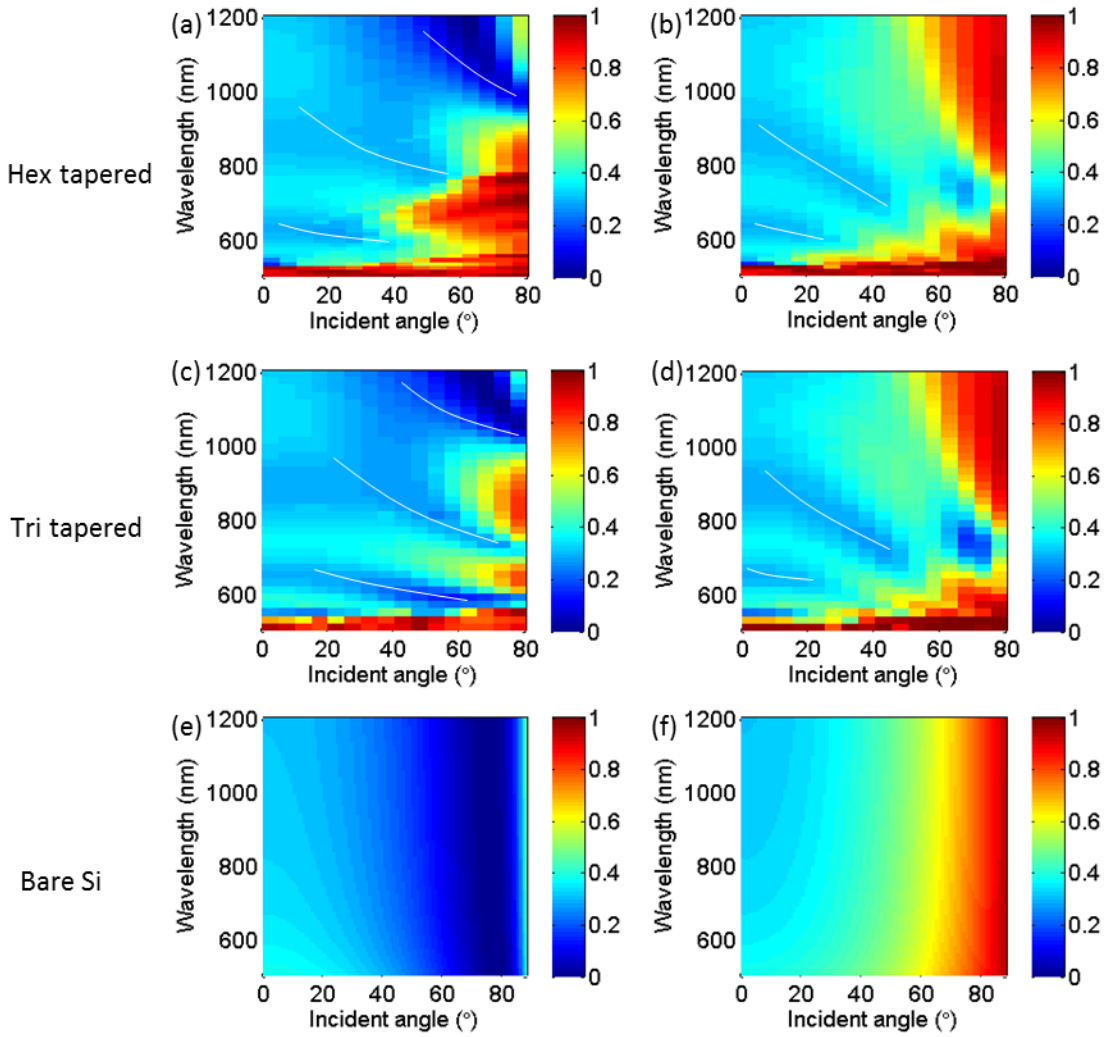

Fig. 2. Simulated reflectance with respect to incident angle and free space wavelength for polarization angles χ of 0° and 90°. (a, b): hexagonal arrays of tapered silicon pillar; (c, d): triangular arrays of tapered silicon pillar. The curved lines represent the diffraction orders. (e, f): bare silicon surface. (a, c, e): $\chi = 0°$; (b, d, f): $\chi = 90°$.

Figures 2(e) and 2(f) present the reflectance of light of the bare air-silicon interface, calculated from the Fresnel formula. It should be noted that when TM ($\chi = 0°$) polarized light impinged on the bare silicon surface, the reflection was small for incident angles at ~75° (Brewster angle). For instance, the reflectance of light was 7×10^{-4}, for $\lambda = 1200$ nm and $\theta = 75°$.

Using the simulated data, the reflectivity of nanopillar arrays with reference to the bare Si substrate was calculated. Figure 3 shows the reflection enhancement factor of the structured silicon surfaces compared with the bare silicon surfaces. It was observed that for TM

polarization, the nanopillar arrays displayed a high reflectance at incidence angles larger than 60°. The light reflection was significantly enhanced (near infinity) at the Brewster angle (~75°) for TM polarized light. Therefore log scale is used in Fig. 3(a) and (c) for better visualization of the complete range of data.

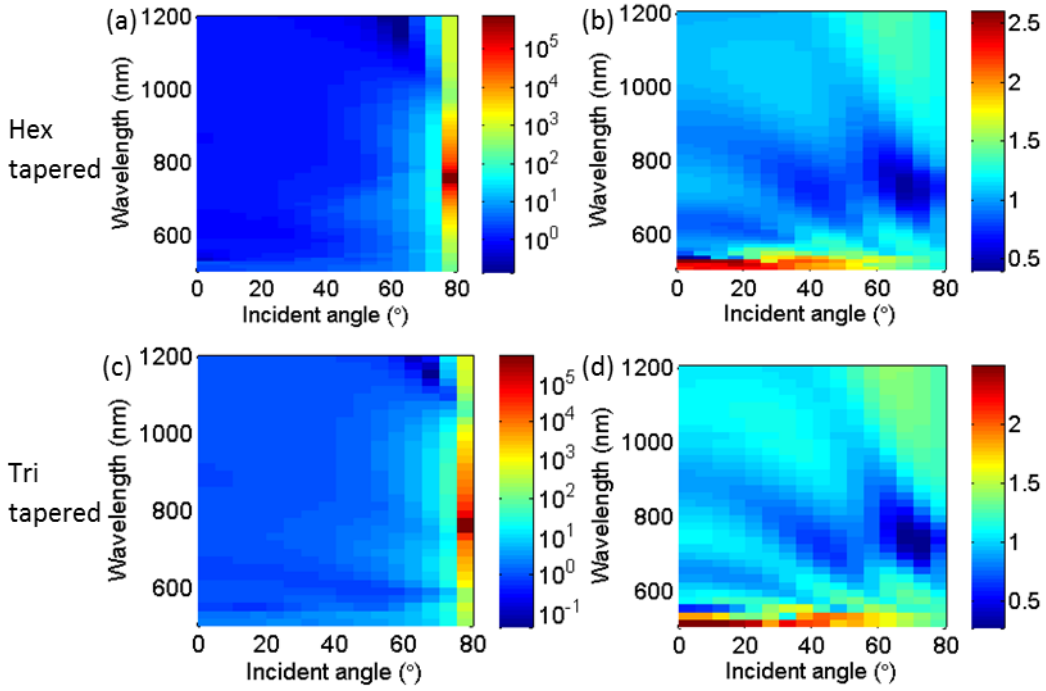

Fig. 3. Simulated reflection enhancement factor for hexagonal [(a, b)] and triangular [(c, d)] arrays of inverse tapered silicon pillars on silicon surfaces for $\chi = 0°$ [(a, c)] and 90° [(b, d)].

The arrays also displayed enhanced reflection for the TE polarized light. This was not as high as the TM reflection since TE light was polarized perpendicular to the Si pillars leading to a reduced interaction of light with the pillars. In TM wave, the light is polarized parallel to the pillars, which act as regular disinclinations for the propagation of light and produce multiple reflections. Another reason for the high reflection at large incidence angles is that light propagating through the arrays and is refracted upward. The inverse tapered nanopillars present a higher refractive index on their tips compared with the bases, which leads to the upwards refraction of light. To confirm the accuracy of the simulation results a series of control simulations were carried out, which are shown in the supplementary material.[7]

The 2D hexagonal and triangular lattice arrays of Si-inverted nanocones were fabricated by first using e-beam lithography to produce a dot array pattern (1 x 1 mm) on the Si substrates. The

pattern was then sputtered with a 200 nm thick tungsten mask followed by the deep reactive etching (DRIE) allowed etching of the substrate.[4,8] Next, the array was exposed to the following gases for one second each, in a succession lasting for 5 min: C_4F_8 for protective layering, SF_6 for etching, and O_2 for removing the SF_6 residues, respectively. Scanning electron micrographs (SEM) (Fig. 4) show well-ordered and periodically patterned Si-inverted nanocones. Due to the small lower radii of the nanopillars, the periodicity was imperfect in some areas of the sample.

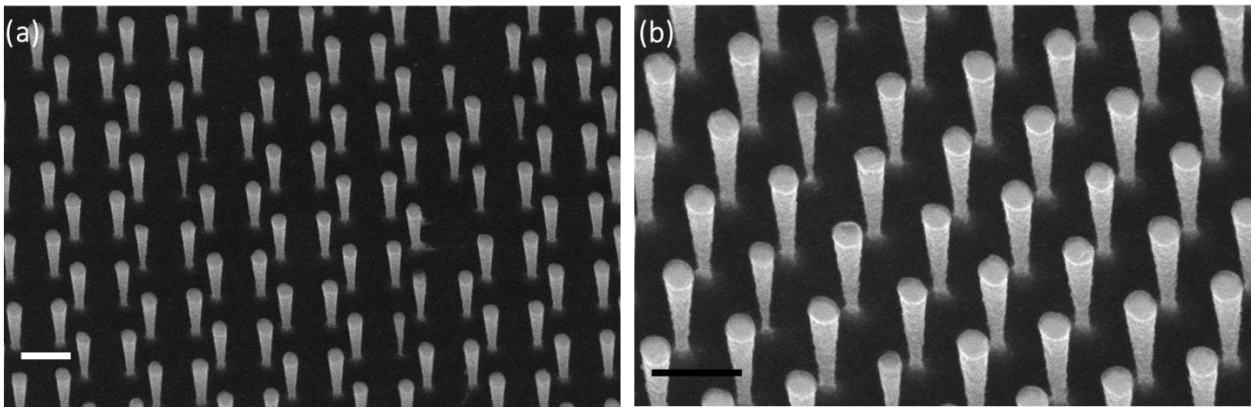

Fig. 4. SEM images of the fabricated arrays of inverted-Si nanocones in (a) hexagonal and (b) triangular lattices. The scale bars = 300 nm.

The enhanced reflection effect displayed by the arrays of inverted nanocones was efficient and could be visually observed upon illumination with a light source (Fig. 5a, b). The images showed a focused spot of a beam of light falling on the bare Si substrates, and subsequently on the hexagonal lattice array of nanocones, while the intensity of light was kept constant. The spot becomes brighter when incident light was directed onto the Si nanocone array, compared with the light directed at a bare Si substrate. The diffraction of light from the array was also studied by shining a 345 nm blue laser normal to the surface of the hexagonal array. The laser light was diffracted into 6 hexagonally localized spots on a transparent hemispherical screen (placed above the sample) (Fig. 5c).[9] The diffraction spots which were at an angle of 60^o from the vertical. The experiment was also repeated with a beam of focused white light, and the diffracted first order light was observed on a screen (Fig. 5d). The diffraction angle increased as the light shifted from short to longer wavelengths, obeying Bragg's law.

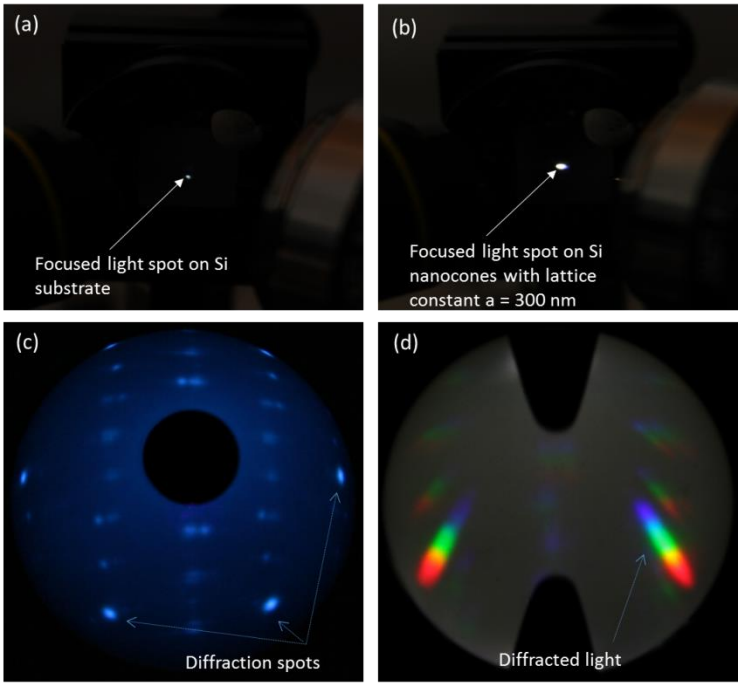

Fig. 5. The focused spot of polarized light illuminating (a) bare Si substrate and (b) the hexagonal array of inverted nanocones. Diffraction of (c) blue laser light and (d) white light from the hexagonal array.

The patterned arrays of Si NCs were also characterized using a spectrophotometer. A white-light source (450-1200 nm, Ocean Optics) was used to illuminate the array. The reflection measurements were performed for both light polarized parallel (TE) and perpendicular (TM) to the Si NCs. The polarization of the white-light beam was selected before the beam was guided onto the sample. The light beam was first collimated and focused onto the sample through a series of microscope objectives to ensure that the incident beam spot size was smaller than the active area of the sample (1×1 mm). A high numerical aperture lens was closely positioned next to the sample to collect the reflected light. The collected beam (500-1150 nm) was then focused into a feed fiber of a spectrophotometer (Ocean Optics 2000) with a resolution of 0.3 nm. Measurements were recorded for an incidence angle of ~70°, since for higher angles the illumination spot size is larger than the Si NCs arrays.

The reflection spectra were recorded for both the triangular and hexagonal array samples. The reflection spectra were normalized with respect to the reference reflection spectra measured from bare Si substrates. The normalized reflectance spectra are in shown Fig. 6. As predicted from the simulation results, the measured spectra showed enhanced reflection from nanopillars arrays and

also the dips associated with the diffraction of light. As also predicted from the simulation results, a larger reflection enhancement was observed on the TM (χ = 0°) mode of light as compared with the TE (χ = 90°). Several diffraction orders were observed as dips in the measured spectra, which represented light that was diffracted at large angles (due to small lattice constant of the arrays) and was not captured by the lens that focused the reflected light into the spectrometer.

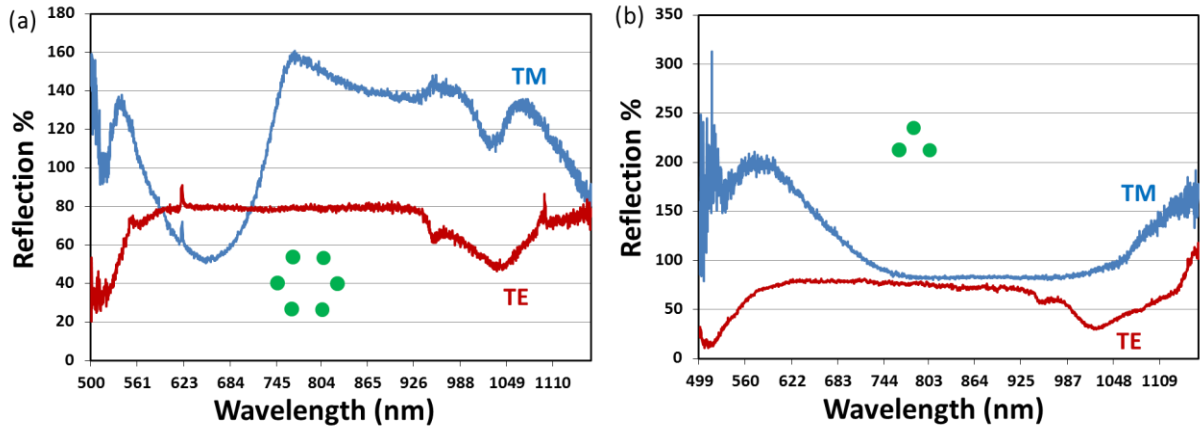

Fig. 6. Reflection spectra for hexagonal (a) and triangular (b) arrays of inverse tapered silicon pillars on silicon surfaces for TM (χ = 0°) and TE (χ = 90°) polarizations.

A maximum reflectance enhancement of ~160% was measured from the hexagonal array and ~200% from the triangular array, both for TM polarization. The reflection spectra also show the theoretically predicted diffracted order dips, which occur as harmonics. For example, for the hexagonal array the first TM dip occurs at ~510 nm and the second order of this is at ~1020 nm. The other major dip is at ~650 nm which has its second order at 1300 nm. However, the location of these dips is not completely consistent with the simulation results. The offsets in the dip locations might be attributed to variation in the incident angles during reflectance measurements. Another for this discrepancy might be the usage of a focused light source since the array was relatively small (1×1 mm). The focused light within the incident beam might impinge onto the arrays at different incident angles, hence potentially causing slight shifts in the reflectance spectra.

In conclusion, we computationally and experimentally studied the reflection and diffraction from periodic hexagonal and triangular arrays of inverse tapered silicon nanopillars. Due to the tapered shape, these nanocone arrays display angle- and polarization-dependent enhanced

reflection, as compared to bare Si substrates. These inverted nanocone arrays can be used for applications in optical filtering, smart windows and photovoltaics to reflect the undesired wavelength regimes.

Acknowledgements

HB would like to thank The Leverhulme Trust for the research funding. QD is supported by Bureau of International Cooperation, Chinese Academy of Sciences (121D11KYSB20130013).

References

[1] Hang Zhou, Alan Colli, Arman Ahnood, Yang Yang, Nalin Rupesinghe, Tim Butler, Ibraheem Haneef, Pritesh Hiralal, Arokia Nathan, and Gehan A. J. Amaratunga, Advanced Materials **21** (38-39), 3919 (2009); Dmitry Chigrin, Andrei Lavrinenko, and Clivia Sotomayor Torres, Opt. Express **12** (4), 617 (2004).

[2] Yung Hung, Jr., San-Liang Lee, and Larry A. Coldren, Opt. Express **18** (7), 6841 (2010).

[3] Jia Zhu, Zongfu Yu, George F. Burkhard, Ching-Mei Hsu, Stephen T. Connor, Yueqin Xu, Qi Wang, Michael McGehee, Shanhui Fan, and Yi Cui, Nano Letters **9** (1), 279 (2008).

[4] Haider Butt, Qing Dai, Ranjith Rajasekharan, Timothy D. Wilkinson, and Gehan A. J. Amaratunga, Applied Physics Letters **99** (13), 133105 (2011).

[5] E.D. Palik, *Handbook of Optical Constants of Solids*. (Elsevier Science, 1998).

[6] Kanghee Won, Ananta Palani, Haider Butt, Philip J. W. Hands, Ranjith Rajeskharan, Qing Dai, Ammar Ahmed Khan, Gehan A. J. Amaratunga, Harry J. Coles, and Timothy D. Wilkinson, Advanced Optical Materials **1** (5), 368 (2013).

[7] See supplementary material at [1] for the control simulation results.

[8] Haider Butt, Qing Dai, Niraj N. Lal, Timothy D. Wilkinson, Jeremy J. Baumberg, and Gehan A. J. Amaratunga, Applied Physics Letters (Under review).

[9] Haider Butt, Tim Butler, Yunuen Montelongo, Ranjith Rajesekharan, Timothy D. Wilkinson, and Gehan A. J. Amaratunga, Applied Physics Letters **101** (25) (2012); Haider Butt, Yunuen Montelongo, Tim Butler, Ranjith Rajesekharan, Qing Dai, Sai G. Shiva-Reddy, Timothy D. Wilkinson, and Gehan A. J. Amaratunga, Advanced Materials **24** (44), OP331 (2012).